

Supporting Information for

Cp\* non-innocence and the implications of ( $\eta^4$ -Cp\*H)Rh intermediates in hydrogenation of CO<sub>2</sub>, NAD<sup>+</sup>, amino-borane, and the Cp\* framework – *a computational study*

Shrinwantu Pal

Coordination Chemistry and Catalysis Unit, Okinawa Institute of Science and Technology  
1919-1 Tancha, Onna-son, Okinawa, 904-0495, Japan

shrinwantu.pal@oist.jp

## 1. Computational Details

Density functional theory (DFT) calculations were performed using the M06L<sup>1,2</sup> functional (with density fitting, using the 'denfit'<sup>2</sup> keyword in Gaussian terminology) and def2-tzvp<sup>3</sup> basis sets for all elements (default ECPs for Rh) as implemented in the Gaussian 16 package.<sup>4</sup> All structures were fully optimized using the SMD<sup>5</sup> solvation model. NBO calculations were performed using the NBO 7.0 package.<sup>6</sup> Connectivity between the transition states and corresponding intermediates on either side were established by means of intrinsic reaction coordinate (IRC) calculations at the same level of theory. Analytical frequency calculations (at 298.15 K and 1 atm.) performed on the resultant geometries conformed to exactly ZERO imaginary frequencies for all ground states and exactly ONE imaginary frequency for the transition states.

Free energies of solutes were corrected for the change in standard states.<sup>7,8</sup> Solubilities of H<sub>2</sub><sup>9</sup> and CO<sub>2</sub><sup>10</sup> at higher pressures were adapted from literature,<sup>9-11</sup> as detailed below. The hydroxide ion as well as transition states for (de)protonation were calculated by adding explicit water molecules.

Gibbs free energies are reported as the sum of solvent-corrected electronic and thermal free energies. All geometries are provided as MOL2 files which can be directly opened in any molecule editor, such as Mercury (<https://www.ccdc.cam.ac.uk>), Avogadro (<https://avogadro.cc>) or Jmol (<http://jmol.sourceforge.net>). Animations corresponding to imaginary frequencies from vibrational analysis are provided as GIF files, while those showing the intrinsic reaction coordinates corresponding to **TS6** as discussed in the main text is provided as a MOV file (**IRC6**).

The following tables tabulate the free energies of all calculated species; additionally, an interactive XLS sheet is also being provided.

## 2. Tables

The solubility of H<sub>2</sub><sup>9</sup> and CO<sub>2</sub><sup>10</sup> at 2 MPa pressure in water are presented in the literature as volume equivalent of the gas (in cc) at STP that dissolves in 1 g of water. Conversion to mol/L yields the solubilities of H<sub>2</sub> and CO<sub>2</sub> as 0.02 M and 0.58 M. On the other hand, the solubility of H<sub>2</sub> at ~ 4MPa in THF<sup>11</sup> is presented in the literature as mole fraction in THF (density = 887 g/L; M<sub>w</sub> = 72.11 g/mol). Conversion to mol/L yields the solubility of H<sub>2</sub> in THF as 0.12 M.

**Table S1: Solubilities of H2 and CO2 at higher pressures**

	Conc. (M)	Notes
H2, 2 MPa in water	0.02	Solubility of H2 in water at 2 MPa H2 pressure is 0.44 cc/g of water
CO2, 2 MPa in water	0.58	Solubility of CO2 in water at 2 MPa CO2 pressure is 14.2 cc/g of water
H2, 4 MPa in THF	0.12	Molefraction solubility of H2 in THF at 4 MPa H2 pressure is 0.00996

Standard state correction<sup>12</sup> is given as: SSC = 0.593\*ln[Concentration(M)/0.0409]. The concentration of bulk solvents water and THF are 55.5 M (c = 1000 g/L ÷ 18 g/mol) and 12.3 M (c = 887 g/L ÷ 72.11 g/mol), respectively. Concentration of DMAB was taken as 4.0 M to reflect experimental conditions reported.<sup>13</sup> The free energy of hydroxide was calculated by explicitly solvating the OH<sup>-</sup> ion by three water molecules to the gas-phase free energy of the OH<sup>-</sup> ion calculated by DFT and further corrected to account for a concentration of 1 M.

**Table S2: Free energy corrections**

	ΔG (DFT) (Hartree)	conc. (M)	Correction (kcal/mol)	ΔGcorrected a.u.	Notes
H2O	-76.452183	55.55	4.28	<b>-76.445366</b>	SSC
H2 (2 MPa in water)	-1.170728	0.02	-0.49	<b>-1.171503</b>	SSC
CO2 (2 MPa CO2 pressure)	-188.657767	0.58	1.57	<b>-188.655259</b>	SSC
OH-(aq)3	-305.309900	-	-	-305.309900	DFT calculated OH- with explicit solvation with three water molecules (aq)
OH-(aq)3, 1 M in water	-305.309900	1.00	1.90	<b>-305.306879</b>	ΔG(solv, 1 M) = ΔG(solvated) + SSC
THF	-232.416333	12.30	3.38	<b>-232.410941</b>	SSC
DMAB	-161.780761	4.00	2.72	<b>-161.776430</b>	SSC
H2 (4 MPa in THF)	-1.172882	0.12	0.65	<b>-1.171845</b>	SSC

**Table S3: Free Energy profile for the formation of 1, 2 and 3 in 1 M aqueous OH-**

Species	$\Delta G$ (Hartree)				SUM (Hartree)	REL (kcal/mol)	Notes
<b>4</b> + H <sub>2</sub> + OH-(aq) <sub>3</sub> + 3 H <sub>2</sub> O	-1071.813508	-1.171503	-305.306879	-229.336097	-1607.627988	0.0	Starting materials
<b>5</b> + 2 OH-(aq) <sub>3</sub> + H <sub>2</sub>	-995.823095	-610.613758	-1.171503		-1607.608357	12.3	Dissociation of OH- from Rh(III)-center of <b>4</b>
<b>6</b> + 2 OH-(aq) <sub>3</sub>	-996.985880	-610.613758			-1607.599638	17.8	Formation of Rh- $\eta^2$ (H <sub>2</sub> ) int.
<b>TS1</b> + H <sub>2</sub> O + OH-(aq) <sub>3</sub>	-1225.835867	-76.445366	-305.306879		-1607.588112	25.0	TS for deprotonation of Rh- $\eta^2$ (H <sub>2</sub> ) fragment
<b>1</b> + 4 H <sub>2</sub> O + OH-(aq) <sub>3</sub>	-996.545022	-305.781463	-305.306879		-1607.633364	-3.4	Formation of Rh(III)-H
<b>TS2</b> + 4 H <sub>2</sub> O + OH-(aq) <sub>3</sub>	-996.517986	-305.781463	-305.306879		-1607.606328	13.6	TS for reductive elimination of the Cp*-H pair
<b>2</b> + 4 H <sub>2</sub> O + OH-(aq) <sub>3</sub>	-996.546434	-305.781463	-305.306879		-1607.634776	-4.3	Formation of Cp*H(endo) Rh(I) complex
<b>TS3</b> + 5 H <sub>2</sub> O	-1225.389695	-382.226829			-1607.616524	7.2	TS for reductive deprotonation of Rh(III)-H
<b>7</b> + 8 H <sub>2</sub> O	-996.080983	-611.562926			-1607.643909	-10.0	Formation of Cp*Rh(I) int. via deprot of Rh-H of <b>1</b>
<b>TS4</b> + 5 H <sub>2</sub> O	-1225.376673	-382.226829			-1607.603502	15.4	TS for protonation of Cp* fragment of <b>7</b> in exo manner
<b>TS5</b> + 5 H <sub>2</sub> O	-1225.372606	-382.226829			-1607.599435	17.9	TS for protonation of the Cp* fragment of <b>7</b> in endo manner
<b>3</b> + OH-(aq) <sub>3</sub> + 4 H <sub>2</sub> O	-996.546882	-305.306879	-305.781463		-1607.635224	-4.5	Formation of Cp*H(exo) Rh(I) int.

Note: free energies of **1**, **2** and **3** relative to **4** are highlighted in purple

**Table S4: Free energy profile for the hydrogenation of CO<sub>2</sub>**

Species	$\Delta G$ (Hartree)				SUM (Hartree)	REL (kcal/mol)	Notes
<b>1</b> + CO <sub>2</sub> + OH-(aq) <sub>3</sub>	-996.545022	-188.655259	-305.306879		-1490.507160	0.0	Rh(III)-H intermediate
<b>TS6</b> + OH-(aq) <sub>3</sub>	-1185.181631	-305.306879			-1490.488510	11.7	TS for direct hydride transfer to CO <sub>2</sub>
<b>5</b> + HCOO- + OH-(aq) <sub>3</sub>	-995.823095	-189.367447	-305.306879		-1490.497421	6.1	Formation of 5-coordinate Rh(III) int. and formate
<b>8</b> + OH-(aq) <sub>3</sub>	-1185.197682	-305.306879			-1490.504561	1.6	Coordination of formate to Rh(III)-center of <b>5</b>
<b>2</b> + CO <sub>2</sub> + OH-(aq) <sub>3</sub>	-996.546434	-188.655259	-305.306879		-1490.508572	-0.9	endo Cp*H intermediate
<b>TS7</b> + OH-(aq) <sub>3</sub>	-1185.143513	-305.306879			-1490.450392	35.6	TS for hydride transfer from endo Cp*H to CO <sub>2</sub>
<b>3</b> + CO <sub>2</sub> + OH-(aq) <sub>3</sub>	-996.546882	-188.655259	-305.306879		-1490.509020	-1.2	exo Cp*H intermediate
<b>TS8</b> + OH-(aq) <sub>3</sub>	-1185.159495	-305.306879			-1490.466374	25.6	TS for hydride transfer from exo Cp*H to CO <sub>2</sub>
<b>4</b> + HCOO- + 3 H <sub>2</sub> O	-1071.813508	-189.367447	-229.336097		-1490.517052	-6.2	Formation of formate and reinstatement of <b>4</b>

**Table S5: Barriers for hydride delivery to NAD<sup>+</sup> from 1, 2 and 3**

Species	$\Delta G$ (Hartree)				SUM (Hartree)	REL (kcal/mol)	Notes
<b>4</b> + HCOO- + NAD <sup>+</sup> + 3 H <sub>2</sub> O	-1071.813508	-189.367447	-456.752617	-229.336097	-1947.269669	0.0	Starting materials
<b>TS9</b> + OH- + CO <sub>2</sub>	-1453.287123	-305.306879	-188.657767		-1947.251769	11.2	TS for direct hydride transfer to NAD <sup>+</sup>
<b>TS10</b> + OH- + CO <sub>2</sub>	-1453.245097	-305.306879	-188.657767		-1947.209743	37.6	TS for hydride transfer from endo Cp*H to NAD <sup>+</sup>
<b>TS11</b> + OH- + CO <sub>2</sub>	-1453.263480	-305.306879	-188.657767		-1947.228126	26.1	TS for hydride transfer from exo Cp*H to NAD <sup>+</sup>

**Table S6: Energy profile for the hydrogenation of the Cp\* framework in the reaction with DMAB in the presence of H2 in THF**

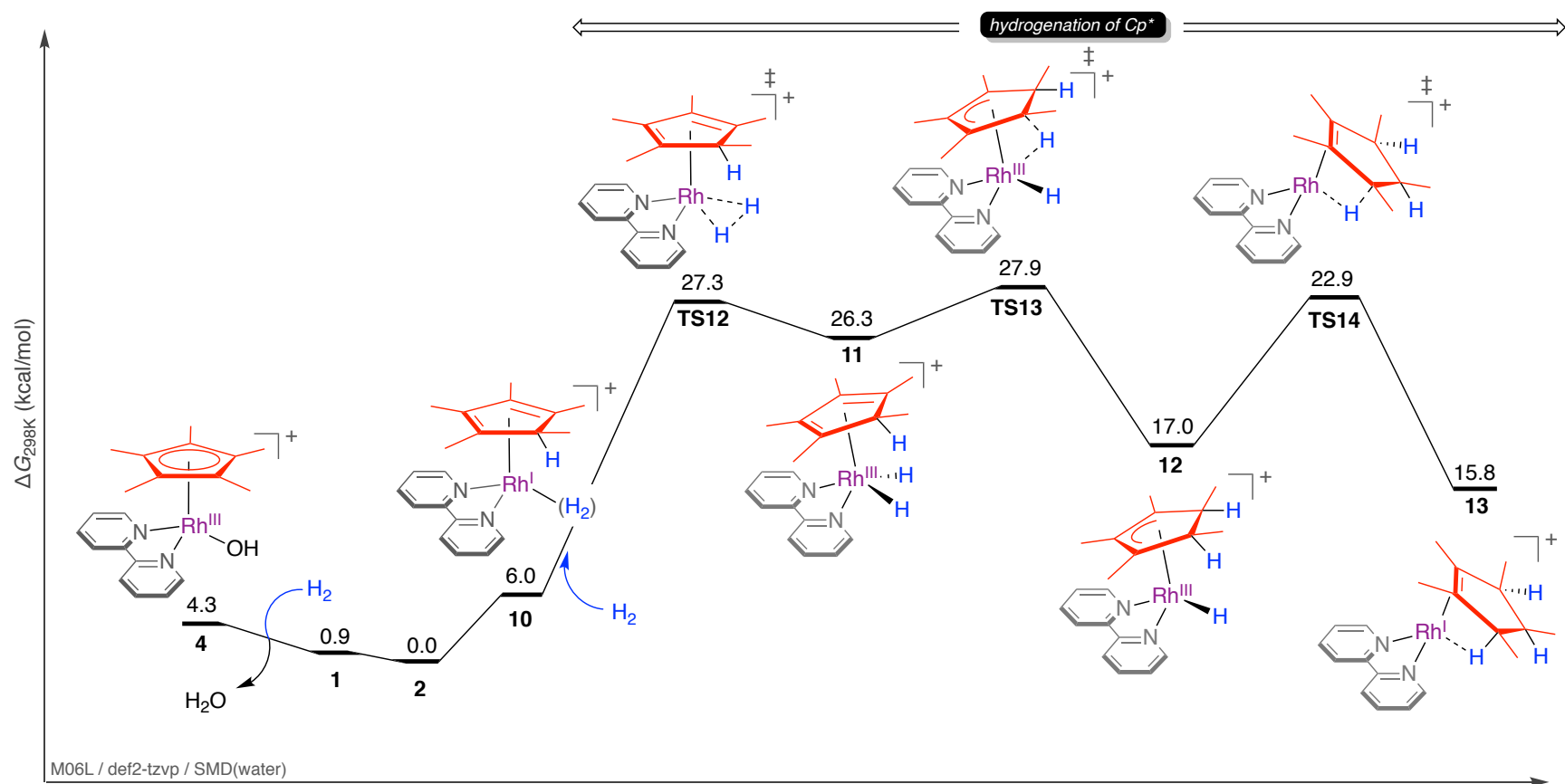
Species	$\Delta G$ (Hartree)			SUM (Hartree)	REL (kcal/mol)	Notes
<b>9'</b> + DMAB + H2	-1228.217017	-161.776430	-1.171845	-1391.165292	12.6	<i>Cp*Rh-THF complex + dimethylamine-borane + H2</i>
<b>1'</b> + Me2NHBH2-THF + H2	-996.555693	-393.457762	-1.171845	-1391.185300	0.0	<i>Formation of Rh(III)-H intermediate and [Me2NH-BH2THF]+</i>
<b>2'</b> + Me2NHBH2-THF + H2	-996.555174	-393.457762	-1.171845	-1391.184781	0.3	<i>Formation of (Cp*H)Rh intermediate</i>
<b>10'</b> + Me2NHBH2-THF	-997.718212	-393.457762		-1391.175974	5.9	<i>Formation of <math>\eta^1</math>-(H2) (Cp*H) Rh intermediate</i>
<b>TS12'</b> + Me2NHBH2-THF	-997.686024	-393.457762		-1391.143786	26.1	<i>TS for oxidative addition of H2</i>
<b>11'</b> + Me2NHBH2-THF	-997.687266	-393.457762		-1391.145028	25.3	<i>Formation of (Cp*H) Rh(III) dihydride</i>
<b>TS13'</b> + Me2NHBH2-THF	-997.684639	-393.457762		-1391.142401	26.9	<i>TS for insertion of Cp*H in Rh(III)-H fragment</i>
<b>12'</b> + Me2NHBH2-THF	-997.697796	-393.457762		-1391.155558	18.7	<i>Formation of <math>\eta^3</math>-allylic Cp*H2 Rh(III)-H intermediate</i>
<b>TS14'</b> + Me2NHBH2-THF	-997.690195	-393.457762		-1391.147957	23.4	<i>TS for C-H reductive coupling</i>
<b>13'</b> + Me2NHBH2-THF	-997.702409	-393.457762		-1391.160171	15.8	<i>Formation of <math>\eta^2</math>-Cp*H3 Rh(I) intermediate</i>

**Table S7: Energy profile for the hydrogenation of the Cp\* framework with H2 in water**

Species	$\Delta G$ (Hartree)			SUM (Hartree)	REL (kcal/mol)	Notes
<b>4</b> + 2 H2	-1071.813508	-2.3430066		-1074.156515	4.3	<i>Cp*Rh-OH complex + 2 H2</i>
<b>1</b> + H2 + H2O	-996.545022	-1.171503	-76.445366	-1074.161891	0.9	<i>Formation of Rh(III)-H intermediate and H2O</i>
<b>2</b> + H2 + H2O	-996.546434	-1.171503	-76.445366	-1074.163303	0.0	<i>Formation of (Cp*H)Rh intermediate</i>
<b>10</b> + H2O	-997.708402	-76.445366		-1074.153768	6.0	<i>Formation of <math>\eta^1</math>-(H2) (Cp*H) Rh intermediate</i>
<b>TS12</b> + H2O	-997.674368	-76.445366		-1074.119734	27.3	<i>TS for oxidative addition of H2</i>
<b>11</b> + H2O	-997.676018	-76.445366		-1074.121384	26.3	<i>Formation of (Cp*H) Rh(III) dihydride</i>
<b>TS13</b> + H2O	-997.673415	-76.445366		-1074.118781	27.9	<i>TS for insertion of Cp*H in Rh(III)-H fragment</i>
<b>12</b> + H2O	-997.690859	-76.445366		-1074.136225	17.0	<i>Formation of <math>\eta^3</math>-allylic Cp*H2 Rh(III)-H intermediate</i>
<b>TS14</b> + H2O	-997.681373	-76.445366		-1074.126739	22.9	<i>TS for C-H reductive coupling</i>
<b>13</b> + H2O	-997.692727	-76.445366		-1074.138093	15.8	<i>Formation of <math>\eta^2</math>-Cp*H3 Rh(I) intermediate</i>

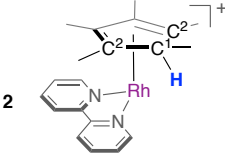
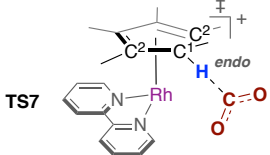
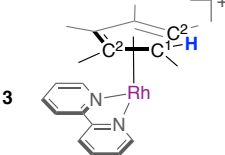
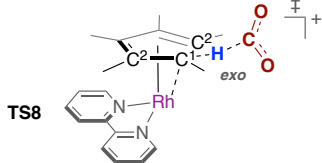
Note: see Scheme S1 below

Scheme S1. Gibbs free energy profile for the hydrogenation of the Cp\* framework in water



### 3. NBO calculations

NBO calculations were performed on **2**, **3** and **TS7** and **TS8**, paying emphasis on the interaction between the Rh, C<sup>1</sup> and H atoms, as shown below.

Species	Donor	Acceptor	$E^{(2)}$ kcal/mol
	Rh-C <sup>2</sup>	$\sigma^*(\text{C}^1\text{-H})$	1.04
	Lp(Rh)	Lv(C <sup>1</sup> )	27.96
	Lp(Rh)	Lv(C <sup>1</sup> )	12.19
	Lp(Rh)	$\sigma^*(\text{C}^1\text{-H})$	1.06
	Lp(C <sup>1</sup> )	$\sigma^*(\text{Rh-C}^2)$	123.08
	Lp(C <sup>1</sup> )	$\sigma^*(\text{Rh-C}^2)$	122.95

According to NBO<sup>6</sup> calculations, **2** exhibits an extremely weak donation ( $E^{(2)} = 1.04$  kcal/mol) of electrons from the Rh-C<sup>2</sup> fragment into the C<sup>1</sup>-H fragment. As the complex departs towards hydride delivery, in **TS7**, filled *d*-orbitals on the Rh-center modestly ( $E^{(2)} = 27.96, 12.19$  kcal/mol) donate electron density into empty orbitals on the C1-atom. It is noteworthy, however, that no interaction involving orbitals of the C<sup>1</sup>-H fragment were detected.

In contrast, **3** exhibits a weak donation of electrons from *d*-orbitals on the Rh-center into the  $\sigma^*(\text{C}^1\text{-H})$  fragment, predisposing it towards C-H cleavage, consistent with the lower energy calculated for **TS8**. Indeed, in **TS8**, the lone pair orbitals on the C1-atom undergo extensive stabilizing overlap ( $E^{(2)} = 123.08, 122.95$  kcal/mol) with the flanking C<sup>2</sup>-atoms. This type of interaction is absent in **TS7**.

#### 4. References

- 1 Y. Zhao and D. G. Truhlar, *Theor. Chem. Acc.*, 2008, **120**, 215–241.
- 2 D. G. Gusev, *Organometallics*, 2013, **32**, 4239–4243.
- 3 F. Weigend and R. Ahlrichs, *Phys. Chem. Chem. Phys.*, 2005, **7**, 3297–3305.
- 4 M. J. Frisch, G. W. Trucks, H. B. Schlegel, G. E. Scuseria, M. A. Robb, J. R. Cheeseman, G. Scalmani, V. Barone, G. A. Petersson, H. Nakatsuji, X. Li, M. Caricato, A. V. Marenich, J. Bloino, B. G. Janesko, R. Gomperts, B. Mennucci, H. P. Hratchian, J. V. Ortiz, A. F. Izmaylov, J. L. Sonnenberg, Williams, F. Ding, F. Lipparini, F. Egidi, J. Goings, B. Peng, A. Petrone, T. Henderson, D. Ranasinghe, V. G. Zakrzewski, J. Gao, N. Rega, G. Zheng, W. Liang, M. Hada, M. Ehara, K. Toyota, R. Fukuda, J. Hasegawa, M. Ishida, T. Nakajima, Y. Honda, O. Kitao, H. Nakai, T. Vreven, K. Throssell, J. A. Montgomery Jr., J. E. Peralta, F. Ogliaro, M. J. Bearpark, J. J. Heyd, E. N. Brothers, K. N. Kudin, V. N. Staroverov, T. A. Keith, R. Kobayashi, J. Normand, K. Raghavachari, A. P. Rendell, J. C. Burant, S. S. Iyengar, J. Tomasi, M. Cossi, J. M. Millam, M. Klene, C. Adamo, R. Cammi, J. W. Ochterski, R. L. Martin, K. Morokuma, O. Farkas, J. B. Foresman and D. J. Fox, *Gaussian 16 Rev. C.01.*, 2016
- 5 A. V. Marenich, C. J. Cramer and D. G. Truhlar, *J. Phys. Chem. B*, 2009, **113**, 6378–6396.
- 6 E. D. Glendening, C. R. Landis and F. Weinhold, *J. Comput. Chem.*, 2019, **40**, 2234– 2241; Citation for the NBO 7 program: NBO 7.0. E. D. Glendening, J. K. Badenhoop, A. E. Reed, J. E. Carpenter, J. A. Bohmann, C. M. Morales, P. Karafiloglou, C. R. Landis, and F. Weinhold, Theoretical Chemistry Institute, University of Wisconsin, Madison, WI (2018).
- 7 R. E. Plata and D. A. Singleton, *J. Am. Chem. Soc.*, 2015, **137**, 3811–3826.
- 8 S. Pal, K. Nozaki, A. N. Vedernikov and J. A. Love, *Chem. Sci.*, 2021, **12**, 2960–2969.
- 9 R. Wiebe and V. L. Gaddy, *J. Am. Chem. Soc.*, 1934, **56**, 76–79.
- 10 R. Wiebe and V. L. Gaddy, *J. Am. Chem. Soc.*, 1940, **62**, 815–817.
- 11 E. Brunner, *J. Chem. Eng. Data*, 1985, **30**, 269–273.
- 12 C. J. Cramer, *Essentials of computational chemistry: theories and models*, John Wiley & Sons, 2013.
- 13 S. Pal, S. Kusumoto and K. Nozaki, *Organometallics*, 2018, **37**, 906–914.